Andreev reflection in nanoscale metal-superconductor devices

Raedt, H. De; Michielsen, K.; Klapwijk, T.M.

Published in:
Physical Review B

DOI:
10.1103/PhysRevB.50.631

Publication date:
1994

PHYSICAL REVIEW B VOLUME 50, NUMBER 1 1 JULY 1994-I

Andreev reflection in nanoscale metal-superconductor devices

H. De Raedt and K. Michielsen
Institute for Theoretical Physics and Materials Science Centre, University of Groningen, Nijenborgh 4, NL-9747 AG Groningen, The Netherlands

T. M. Klapwijk
Department of Applied Physics and Material Science Centre, University of Groningen, Nijenborgh 4, NL-9747 AG Groningen, The Netherlands

(Received 7 April 1994)

Computer simulation is used to study Andreev reflection in nanoscale normal-metal–superconductor devices. Back-focusing of hole waves through quantum point contacts is demonstrated. The electron-hole conversion efficiency is shown to depend on the diffraction of the electron wave at the quantum point contact.

Present-day technology has opened the possibility of studying superconducting transport in mesoscopic conductors. For superconductors several length scales play a role. In treatments of inhomogeneous superconductors such as normal-metal–superconductor (N-S) devices it is usually assumed that the Fermi wavelength λ_F is much shorter than the BCS coherence length and the London penetration depth. If the relevant dimensions of the N-S device are of the same order of magnitude as λ_F, the physics on the scale of λ_F can be described by the Bogoliubov–de Gennes equations.[1] These equations have recently been used to study a superconducting quantum point contact, i.e., a contact with a width on the scale of λ_F. It was predicted that the supercurrent carried by the contact increases stepwise with increasing width in much the same way as the normal conductance increases.[2]

A very elegant way to study Andreev-reflection[3,4] in the classical ballistic limit has been introduced by Benistant *et al.*[5] A point contact is placed on a very pure, silver crystal which is backed by a superconducting lead film, as depicted in Fig. 1(a). Electrons emitted by the contact travel ballistically to the superconductor, where they are converted into a hole which retraces the path of the incoming electron and is absorbed by the point contact leading to an enhanced conductance of the point contact. The enhanced conductance as a function of voltage across the emitting contact is a direct measure of the energy-dependent Andreev reflection coefficient at the Ag-Pb interface.

In this paper we present a theoretical analysis of nanoscale N-S devices. The relevant length scales in such devices are of the order of a few λ_F. Accordingly, a description in terms of (semi-) classical ballistic transport cannot be used. A calculation of the charge (electron and hole) transport through the device requires a full quantum-mechanical treatment of the problem. We assume a two-dimensional electron gas with a very high mobility. A quantum point contact (QPC) with a width $W \approx \lambda_F$ is positioned in front of a superconductor [see Fig. 1(b)]. Part of the electron wave passes through the constriction, the remaining part being reflected. The electron wave leaving the QPC is scattered in various directions. At the N-S interface the expanding electron wave is Andreev reflected. The interplay of the diffraction of the electron (and hole) wave by the QPC and the Andreev mechanism is of much less importance in one-dimensional mesoscopic N-S junctions[6] than it is in the two-dimensional devices studied here.

The results presented below have been obtained from the numerically exact solution of the time-dependent Bogoliubov–de Gennes equations[1,7]

$$i\hbar\frac{\partial}{\partial t}\begin{pmatrix}\psi(\mathbf{r},t)\\ \phi(\mathbf{r},t)\end{pmatrix}=\begin{pmatrix}\frac{1}{2m^*}(\mathbf{p}-e\mathbf{A})^2+V(\mathbf{r})-E_F & \Delta(\mathbf{r})\\ \Delta^*(\mathbf{r}) & -\frac{1}{2m^*}(\mathbf{p}+e\mathbf{A})^2-V(\mathbf{r})+E_F\end{pmatrix}\begin{pmatrix}\psi(\mathbf{r},t)\\ \phi(\mathbf{r},t)\end{pmatrix}, \tag{1}$$

where $\psi(\mathbf{r},t)$ and $\phi(\mathbf{r},t)$ denote the electron and hole wave function, respectively, m^* is the effective mass, $\mathbf{p}$ is the momentum operator, e is the charge, $\mathbf{A}=\mathbf{A}(\mathbf{r})$ is the vector potential corresponding to an external magnetic field, $V(\mathbf{r})$ is the potential defining the geometry of the device, E_F is the Fermi energy of the electron gas, and $\Delta(\mathbf{r})$ is the gap function (pair potential) which is chosen to be real.

Simulation of a particular device consists of specifying the potential $V(\mathbf{r})$, the gap $\Delta(\mathbf{r})$ (i.e., the geometry of the device), and the vector potential $\mathbf{A}(\mathbf{r})$, setting up the initial

0163-1829/94/50(1)/631(4)/$06.00

state [i.e., an electron wave function $\psi(\mathbf{r},t=0)$ normalized to one, and $\phi(\mathbf{r},t=0)=0$ because there is no hole at $t=0$], and solving Eq. (1) for times as long as needed to obtain the physically relevant behavior. From the time-dependent electron-hole wave function all physically relevant information can be extracted. In addition, much insight into the behavior of the electron and hole wave can be obtained by simply looking at the time development of the probability distribution.

The numerical method that we employ to compute the solution of Eq. (1) is based on Suzuki's fractal decomposition of the time step operator[8] and is described elsewhere.[9] The algorithm is correct up to fourth order in both the time step τ and the mesh size δ and is unconditionally stable, accurate, and efficient. For all practical purposes our results are numerically exact. A typical simulation run takes approximately 13 h of CPU time on a CRAY YMP, using a grid of 1024×513 points, $\delta=\lambda_F/10$, $\tau=0.03125\hbar/E_F$ where E_F is the Fermi energy, and 8192 time steps.

The results reported below are for a device of dimensions 3.4 μm$\times$1.7 μm with the following characteristics: $E_F=21$ meV, $m^*=0.067m_e$, $\Delta=\Delta(r)=0.067E_F$ (unless explicitly stated otherwise), and $\lambda_F=335$ Å. These values apply to GaAs heterostructure devices and superconducting Nb. For simplicity we will assume an idealized model system in which the Fermi levels and the effective masses in the metal and the superconductor are the same. The (ideal) QPC is represented by rectangular potential barriers of height $100E_F$. The vector potential is taken to be $\mathbf{A}=\mathbf{A}(x,y)=(-\int_0^y B_z(x,y')dy',0,0)$ corresponding to a magnetic field $\mathbf{B}=(0,0,B_z(x,y))$ perpendicular to the plane of motion.[9] Inside the superconductor $\mathbf{B}=\mathbf{0}$. For practical purposes, it is expedient to express energies and distances in units of E_F and λ_F, respectively, and we will do so in the sequel.

According to the standard one-dimensional analysis, perfect Andreev scattering, i.e., 100% conversion of electrons into holes, requires that $|E|\ll\Delta$ where E is the energy of the incoming electron wave relative to E_F, and that $\Delta\ll E_F$.[3,4] In a simulation, the initial wave packet is always confined to a finite region in space and therefore its spread in energy $\sigma_E\neq0$. Accordingly, (nearly) perfect Andreev scattering demands that $\sigma_E\ll\Delta\ll E_F$, conditions that can only be met by using simulation boxes not smaller than the size indicated above and a wave packet which is as broad as possible. A systematic simulation study for devices without QPC's (not shown) reveals that if the widths of the initial, normalized Gaussian wave packets $\sigma_x=\sigma_y\geq10\lambda_F$, more than 99% of the electron intensity returns as hole intensity. From an experimental viewpoint this is an acceptable conversion level.

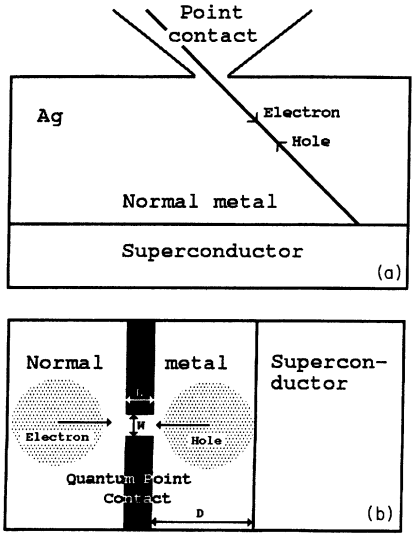

FIG. 1. Layout of the experimental setup to study Andreev reflection. (a) Classical ballistic transport, (b) quantum ballistic transport.

The gaps of conventional superconductors, e.g., Nb compounds, satisfy the condition $\Delta\ll E_F$. In some of the high-T_c cuprates $\Delta\approx0.1E_F$.[10] Therefore, but mainly out of curiosity, it is of interest to solve the Bogoliubov–de Gennes equations for the case where Δ is of the same order of magnitude as E_F. A typical result is shown in Fig. 2 where we have taken $\Delta=E_F$. The energy of the incident electron $E=0$ and $\sigma_x=\sigma_y=10\lambda_F$. Part of the electron wave is reflected instead of converted into hole intensity. Only 80% of the incident electron intensity is returning as hole intensity.

For the present purposes the initial Gaussian wave packet that we use is a very good approximation to a plane wave. Accordingly, an approximate solution of (1) can also be obtained by reducing the two-dimensional problem to a one-dimensional time-independent scattering problem (see below). The solution of the resulting 4×4 scattering matrix problem predicts that about 17% of the electron intensity will be reflected at the interface, in fair agreement with the simulation result (20%). It is important to recognize that the theory given in Refs. 3 and 4 cannot be used to compute this intensity because this theory is only valid in the Andreev limit $\Delta\ll E_F$.

Simulation results for several N-S QPC devices with $\Delta=0.067E_F$, $W=1.6\lambda_F$, and $L=5\lambda_F$ [see Fig. 1(b) for the layout] are shown in Figs. 3–5. In all cases the electron wave packet starts from the left of the QPC, in the direction perpendicular to the interface, and is partially reflected by the QPC. The momenta and energies of all initial wave packets are $|k|=k_F=2\pi/\lambda_F$ and $E=0$, respectively. The part of the electron wave that emerges from the QPC is spreading out rapidly while it moves towards the N-S interface. The occurrence of diffraction is obviously related to the dimensions of the QPC and is absent in the case of classical ballistic transport.[5] In the superconductor, (part of) the electron wave is converted into a hole wave. The hole wave travels to the left and upon leaving the superconductor, is focused back into the constriction.

According to the common lore, quantum mechanics forces wave packets to expand, not to contract. However, hole waves generated by the Andreev mechanism clearly do contract if the electron wave that caused the hole wave was expanding. This feature is implicit in the Bogoliubov–de Gennes equations (1). From (1), it immediately follows that a hole moves exactly like an electron, except that it moves backward in time with a slightly different absolute value of the momentum normal to the interface.[11] The presence of an external magnetic field breaks the electron-hole symmetry and indeed, our simulations (not shown) demonstrated that

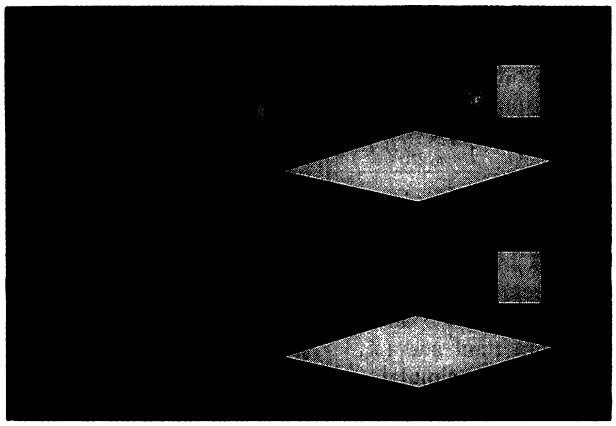

FIG. 2. Two views of a snapshot of the electron (upper part) and hole (lower part) intensity taken at $t=160\hbar/E_F$ for a hypothetical superconductor with gap $\Delta=E_F$. Both the electron and hole wave are moving to the left. Initially, at $t=0$, the electron wave moves to the right, in the direction perpendicular to the interface. Normal metal: dark gray area; superconductor: light gray area.

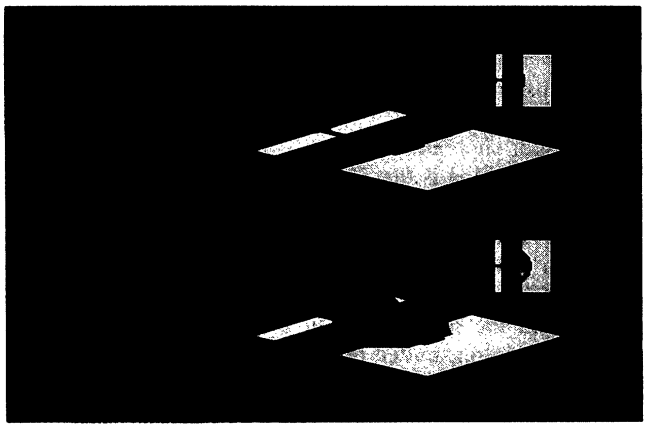

(a)

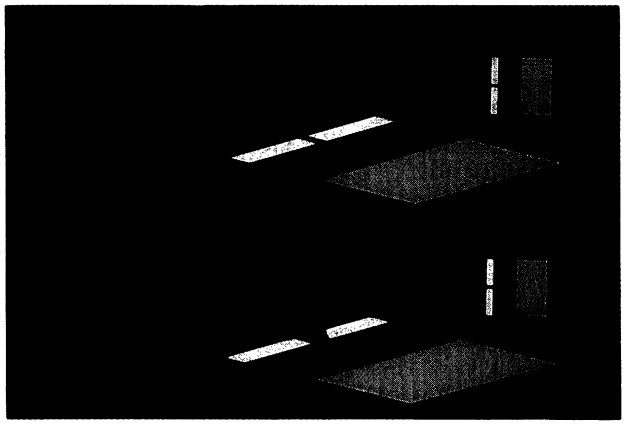

(b)

FIG. 3. Snapshots of the electron (upper part) and hole (lower part) intensity taken at different times. (a) $t=160\hbar/E_F$; (b) $t=256\hbar/E_F$. Normal metal: dark gray area; superconductor: light gray area; quantum point contact: white structure. Device parameters [see Fig. 1(b)]: $\Delta=0.067E_F$, $D=20\lambda_F$, $W=1.6\lambda_F$, $L=5\lambda_F$. Intensities left and right of the QPC are scaled differently for visualization purposes.

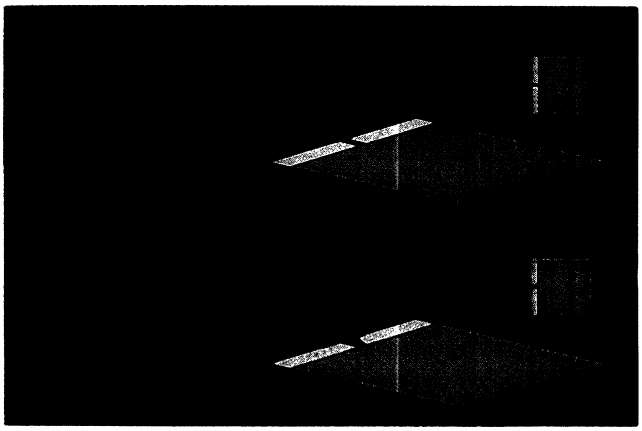

FIG. 4. Same as Fig. 3(b) except that $D=\lambda_F$.

then there will be no back-focusing of the hole into the QPC.

The back-focusing of the hole is most clearly demonstrated in Figs. 3(a) and 3(b) where we show the electron and hole intensity at different times t. For visualization purposes, the intensities at the left- and right-hand side of the exit plane of the QPC are scaled differently. Therefore, Fig. 3(b) gives the impression that there is still a considerable amount of electron (hole) intensity between the QPC and the N-S interface but in fact, the integrated intensity in this part of the device is very small and therefore negligible. The back-focusing itself does not depend on the distance D between the QPC and the N-S interface, as shown in Fig. 4. However, for the device considered here, D is also of the order of λ_F and may be expected to have an influence on the electron-hole conversion efficiency.

Results for the electron and hole current through devices with different D [see Fig. 1(b)] are given in Table I. For small D/λ_F, the conversion of electrons into holes is close

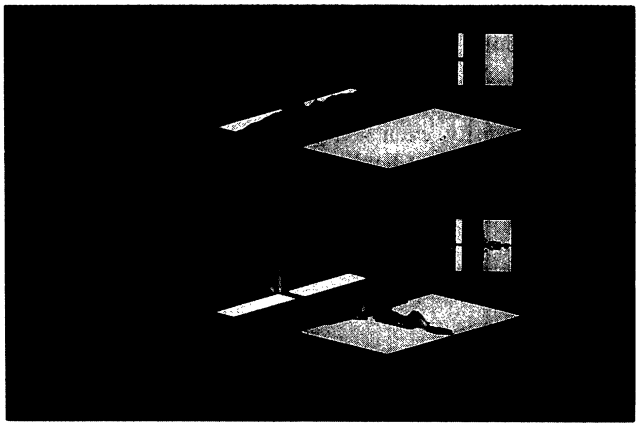

FIG. 5. Same as Fig. 3(b) except that at the N-S interface, a tunnel barrier of width $1\lambda_F$ and height $1.2E_F$ is present. The hole (electron) intensity in the superconductor is larger (smaller) than in the region between the QPC and the tunnel barrier. For visualization purposes the hole and electron intensities at the left- and right-hand side of the exit plane of the QPC are all normalized to one, giving the false impression that there is no hole intensity between the QPC and N-S interface.

TABLE I. Electron (J_e) and hole (J_h) current through the QPC, for the devices shown in Figs. 2–4. Currents in units of $J_0=\hbar k_F/m^*$.

	$D=\lambda_F$	$D=5\lambda_F$	$D=20\lambda_F$
J_e/J_0	1.02	1.05	1.05
J_h/J_0	0.99	0.98	0.91
$(J_e+J_h)/J_e$	1.97	1.93	1.87

to perfect: The third row of Table I indicates that only 1.5% is missing [the theoretical limit is $(J_e+J_h)/J_e=2$]. The loss of conversion efficiency increases with D. For $D=20\lambda_F$ this efficiency is reduced by approximately 6%. The dependence on D of the conversion efficiency is directly related to the diffraction that takes place at the exit plane of the QPC and cannot be accounted for by the standard theory of Andreev reflection.[3,4]

A simple, approximate theory for this phenomenon can be constructed as follows. First consider an infinitely long N-S interface (without QPC) and a plane (electron) wave incident on the interface. The angle of incidence (measured with respect to the normal on the interface) will be denoted by θ. For this geometry Eq. (1) can be reduced to a one-dimensional problem by substituting $\psi(r,t)=f(x)\exp[i(k_y y-Et/\hbar)]$ and $\phi(r,t)=g(x)\exp[i(k_y y-Et/\hbar)]$ yielding

$$\begin{pmatrix} \frac{p_x^2}{2m^*}-\mu^* & \Delta(x) \\ \Delta(x) & -\frac{p_x^2}{2m^*}+\mu^* \end{pmatrix} \begin{pmatrix} f(x) \\ g(x) \end{pmatrix} = E \begin{pmatrix} f(x) \\ g(x) \end{pmatrix}, \tag{2}$$

where the effective chemical potential $\mu^*=E_F-(2m^*)^{-1}\hbar^2k_y^2$. Solving Eq. (2) by the standard wave matching method but without making the usual approximations[3,4] yields the intensity of the reflected holes $R_h=R_h(\mu^*,\Delta)$. For $|k|=k_F$, $\mu^*=E_F\cos^2\theta$.

Diffraction by the QPC leads to an angle dependence of the hole intensity, even if the direction of the incident electron wave is perpendicular to the interface. Adopting the standard expression for the angular distribution $P(\theta)=[\sin(\pi W\sin\theta)/\pi W\sin\theta]^2$ of the electron wave leaving the slit (the QPC) of width W we estimate the hole current transmitted through the QPC device [see Fig. 1(b)] for $D\to\infty$ from

$$\frac{J_h}{J_e}=\frac{\int_{-\pi/2}^{\pi/2}d\theta\, P(\theta)R_h(E_F\cos^2\theta,\Delta)\cos\theta}{\int_{-\pi/2}^{\pi/2}d\theta\, P(\theta)}. \tag{3}$$

Numerical evaluation of the right-hand side of Eq. (3) for $W=1.6\lambda_F$ and $\Delta/E_F=0.067$ yields $(J_e+J_h)/J_e\approx 1.91$, in fair agreement with the simulation result for large D (see Table I). For $D=0$ and normal incidence diffraction effects are unimportant and $(J_e+J_h)/J_e=2$, in reasonable agreement with the simulation data for small D. Thus, due to diffraction at the QPC, the electron-hole conversion efficiency changes with D.

Additional simulations[12] lead to the conclusion that the back-focusing phenomenon itself is extremely robust with respect to changes of device characteristics, such as the gap Δ (not shown), distance between the QPC and the N-S interface (Fig. 4), width of the QPC (not shown), idealness of the interface (Fig. 5), corrugations of the interface (not shown), the angle of incidence of the incoming electron wave (not shown), the presence of impurities in the region between the QPC and the N-S interface (not shown), etc. On the other hand, on the basis of the arguments given above, the electron-hole conversion efficiency may be expected to depend on specific device properties and this is also corroborated by our simulation data.

Our conclusion is that in the absence of a magnetic field, the properties of (ideal) nanoscale N-S devices cannot entirely be described by the standard theory of Andreev reflection[3,4] but can still be "predicted" in terms of the angular distribution of the electron wave impinging on the interface and the notion that all hole intensity entering the metal will be transmitted through the QPC.

We are indebted to N. García for pointing out several errors in the first version of the paper. We have profited from stimulating discussions with P. de Vries and B. J. van Wees. This work is partially supported by the Stichting voor Fundamenteel Onderzoek der Materie (FOM), which is financially supported by the Nederlandse Organisatie voor Wetenschappelijk Onderzoek (NWO), the Stichting Nationale Computer Faciliteiten (NCF), and EEC project ERBCHRXCT930127.

[1] P. G. de Gennes, *Superconductivity of Metals and Alloys* (McGraw-Hill, New York, 1975).

[2] C. W. J. Beenakker and H. van Houten, Phys. Rev. Lett. **66**, 3056 (1991).

[3] A. F. Andreev, Zh. Eksp. Teor. Fiz. **46**, 1823 (1964) [Sov. Phys. JETP **19**, 1228 (1964)].

[4] G. E. Blonder, M. Tinkham, and T. M. Klapwijk, Phys. Rev. B **25**, 4515 (1982).

[5] P. A. M. Benistant, A. P. van Gelder, H. van Kempen, and P. Wyder, Phys. Rev. B **32**, 3351 (1985).

[6] R. A. Riedel and P. F. Bagwell, Phys. Rev. B **48**, 15 198 (1993).

[7] R. Kümmel, Z. Phys. **218**, 472 (1969); see also W. N. Mathews, Jr., Phys. Status Solidi B **90**, 327 (1978).

[8] M. Suzuki, J. Math. Phys. **32**, 400 (1991).

[9] H. De Raedt and K. Michielsen, Comput. Phys. (to be published).

[10] Z.-X. Shen *et al.*, Phys. Rev. Lett. **70**, 1553 (1993).

[11] S. Hofmann and R. Kümmel, Z. Phys. B **84**, 237 (1991).

[12] A VHS video tape or MultiMedia presentation for PC's running Windows 3.1, containing computer animations that show the time development of the electron and hole waves for many different cases may be obtained by contacting one of the first two authors.

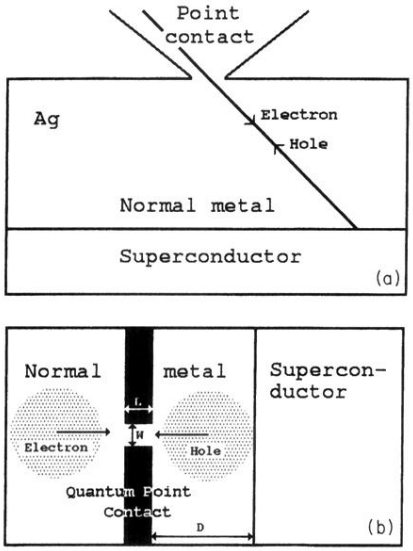

FIG. 1. Layout of the experimental setup to study Andreev reflection. (a) Classical ballistic transport, (b) quantum ballistic transport.

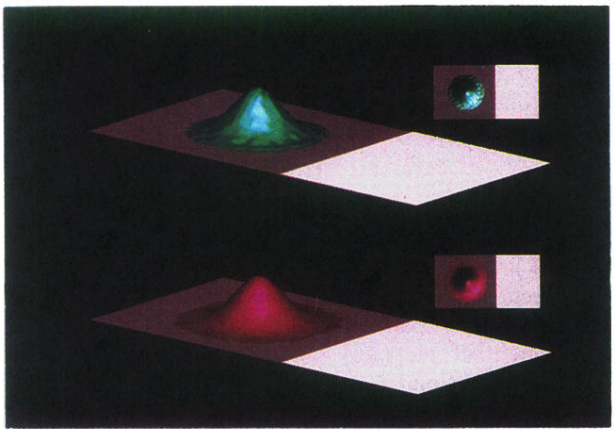

FIG. 2. Two views of a snapshot of the electron (upper part) and hole (lower part) intensity taken at $t = 160\hbar/E_F$ for a hypothetical superconductor with gap $\Delta = E_F$. Both the electron and hole wave are moving to the left. Initially, at $t = 0$, the electron wave moves to the right, in the direction perpendicular to the interface. Normal metal: dark gray area; superconductor: light gray area.

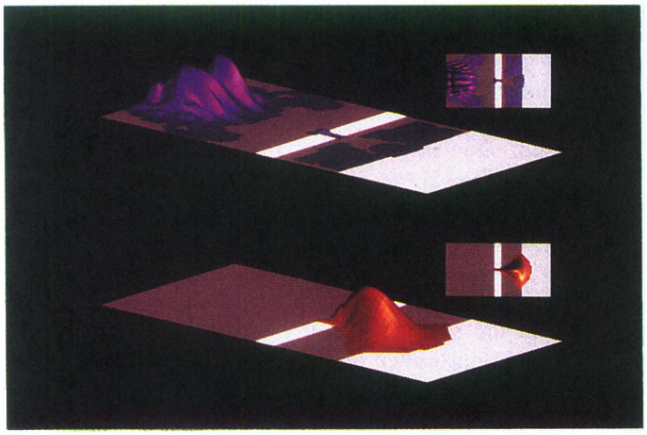

(a)

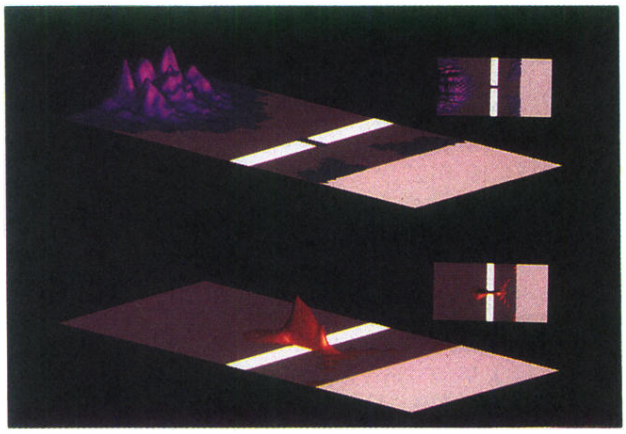

(b)

FIG. 3. Snapshots of the electron (upper part) and hole (lower part) intensity taken at different times. (a) $t=160\hbar/E_F$; (b) $t=256\hbar/E_F$. Normal metal: dark gray area; superconductor: light gray area; quantum point contact: white structure. Device parameters [see Fig. 1(b)]: $\Delta=0.067E_F$, $D=20\lambda_F$, $W=1.6\lambda_F$, $L=5\lambda_F$. Intensities left and right of the QPC are scaled differently for visualization purposes.

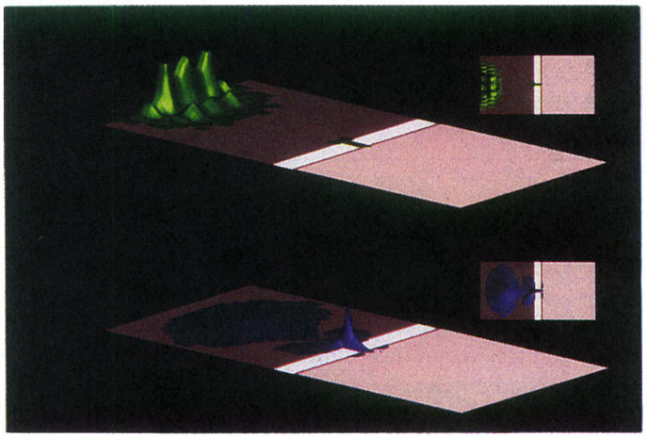

FIG. 4. Same as Fig. 3(b) except that $D = \lambda_F$.

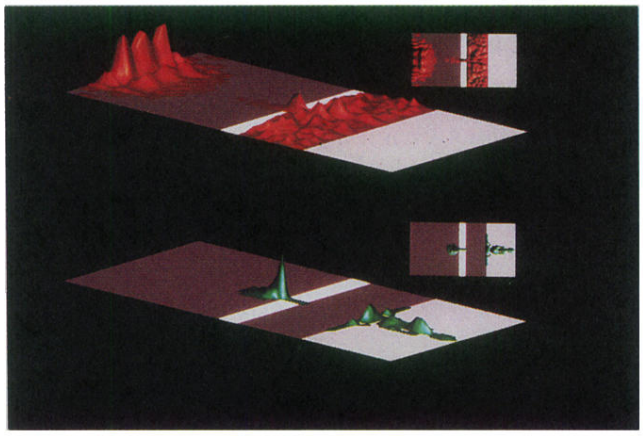

FIG. 5. Same as Fig. 3(b) except that at the N-S interface, a tunnel barrier of width $1\lambda_F$ and height $1.2E_F$ is present. The hole (electron) intensity in the superconductor is larger (smaller) than in the region between the QPC and the tunnel barrier. For visualization purposes the hole and electron intensities at the left- and right-hand side of the exit plane of the QPC are all normalized to one, giving the false impression that there is no hole intensity between the QPC and N-S interface.